Matrix Photochemistry, Photoelectron Spectroscopy, Solid-Phase Structure, and Ring Strain Energy of β-Propiothiolactone

Nahir Y. Dugarte,[†] Mauricio F. Erben,*[,†,#] Rosana M. Romano,[†,#] Roland Boese,[‡] Mao-Fa Ge,[§] Yao Li,[§] and Carlos O. Della Védova*[,†,⊥,#]

CEQUINOR (UNLP-CONICET, CCT-La Plata), Departamento de Química, Facultad de Ciencias Exactas, Universidad Nacional de La Plata, CC 962 (1900), La Plata, República Argentina, Institut für Anorganische Chemie, Universität Duisburg-Essen, Universitätsstrasse 5-7, D-45117 Essen, Germany, State Key Laboratory for Structural Chemistry of Unstable and Stable Species, Institute of Chemistry, Chinese Academy of Sciences, Beijing 100080, China, and LaSeISiC (CIC-UNLP-CONICET), Departamento de Química, Facultad de Ciencias Exactas, Universidad Nacional de La Plata, Camino Centenario y 508, Gonnet, República Argentina

Received: December 30, 2008; Revised Manuscript Received: February 5, 2009

The four-membered heterocyclic β-propiothiolactone compound was isolated in a low-temperature inert Ar matrix, and the UV−visible ($200 \leq \lambda \leq 800$ nm) induced photochemistry was studied. On the basis of the IR spectra, the formation of methylketene ($CH_3CH{=}C{=}O$) was identified as the main channel of photodecomposition. The formation of ethene and thiirane, with the concomitant elimination of OCS and CO, respectively, was also observed as minor decomposition channels. The valence electronic structure was investigated by HeI photoelectron spectroscopy assisted by quantum chemical calculations at the OVGF/6-311++G(d,p) level of theory. The first three bands at 9.73, 9.87, and 12.06 eV are ascribed to the n''_S, n'_O, and $\pi''_{C=O}$ orbitals, respectively, denoting the importance of the −SC(O)− group in the outermost electronic properties. Additionally, the structure of a single crystal, grown in situ, was determined by X-ray diffraction analysis at low temperature. The crystalline solid [monoclinic system, *P*21/*c*, $a = 8.1062(1)$ Å, $b = 10.3069(2)$ Å, $c = 10.2734(1)$ Å, $\beta = 107.628(1)°$, and $Z = 8$] consists of planar molecules arranged in layers. The skeletal parameters, especially the valence angles [∠C2−C1−S = 94.55(7)°, ∠O=C−C = 134.20(11)°, ∠C−S−C = 77.27(5)°], differ from those typically found in acyclic thioester compounds, suggesting the presence of strong strain effects. The conventional ring strain energy was determined to be 16.4 kcal/mol at the G2MP2 level of calculation within the hyperhomodesmotic model.

Introduction

Thiolactones are cyclic esters of thiocarboxylic acids containing a 1-thiocycloalkan-2-one structure. Thiolactones are very interesting molecules in biological terms; the most significant example is the five-membered cyclic homocysteine thiolactone molecule (DL-2-amino-4-mercaptobutyric acid 1,4-thiolactone).[1−3] Moreover, it is well-known that sulfur-containing compounds play an important role in flavor chemistry.[4] Sensory characteristics of γ- and δ-alquil-substituted thiolactones have been evaluated,[5] the odor threshold depending on the ring size and chain length.

Simple non- or alkyl-substituted thiolactones have been the subject of a vast and still-growing number of studies. Structural[6−9] and vibrational[10] analyses as well as kinetics aspects[11] and NMR[12] properties have been studied by experimental and theoretical methods.

The photochemistry of small ring size heterocyclic compounds was studied by several authors.[13,14] Very recently, the UV-induced photochemistry of 2(5*H*)-furanone and 2(5*H*)-thiophenone in low-temperature inert argon matrixes was investigated, and the reaction products were identified by FTIR spectroscopy.[15,16] The unimolecular thermal decomposition of γ-butyrolactone and γ-butyrothiolactone has been studied in a flow system by using HeI photoelectron spectroscopy and quantum chemical calculations.[17,18] For the sulfur-containing heterocycle, decarbonylation and decarboxylation pathways (Scheme 1) are the main and minor decomposition channels, respectively. Interestingly, the opposite trend is found for the oxygen analogues, and γ-butyrolactone pyrolysis is found in the gas-phase mainly via decarboxylation. Further theoretical studies for γ-butyrothiolactone showed that the calculated reaction profile for decarbonylation is favored over decarboxylation by 6.16 kcal/mol within the UMP4/6-31G(d,p)//UHF/6-31G(d,p) method. It was suggested[19] that a low conjugative interaction between the carbonyl group and the vicinal sulfur atom is present in γ-butyrothiolactone. This lack of electronic resonance should favor decarbonylation processes.

SCHEME 1

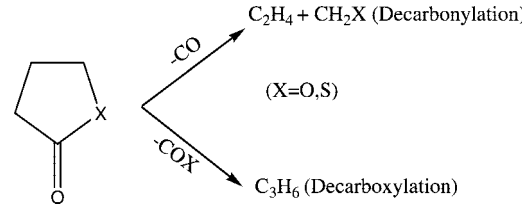

* To whom correspondence should be addressed. Tel/Fax: +54-221-4259485. E-mail: erben@quimica.unlp.edu.ar (M.F.E.); carlosdv@quimica.unlp.edu.ar (C.O.D.V.).
† CEQUINOR (UNLP-CONICET, CCT-La Plata), Universidad Nacional de La Plata.
‡ Universität Duisburg-Essen.
§ Chinese Academy of Sciences.
⊥ LaSeISiC (CIC-UNLP-CONICET), Universidad Nacional de La Plata.
CONICET-La Plata, Member of the Carrera del Investigador del CONICET, República Argentina.

10.1021/jp811480v CCC: $40.75
Published on Web 03/20/2009

On the other hand, the products formed in the pyrolysis of lactones strongly depend on the size of the ring. Pyrolysis ($T \approx 520$ °C) of ring size lactones larger than six atoms promotes elimination reactions to yield unsaturated acids.[20] In contrast, four-[21−24] and five-membered[25] β-lactones decompose at lower temperatures ($T = 140-160$ °C) into carbon dioxide and the corresponding alkene via a concerted pathway.[26] To the best of our knowledge, no studies on the four-membered sulfur analogues have been reported previously.

These observations suggest that several factors influence the stability of these heterocyclic compounds. Indeed, differences between oxo- and thiolactones are expected since the electronic properties of the −C(O)X− (X = O, S) group should have a key role in the decomposition channels. Furthermore, it should be also noted that the cyclic arrangement forces the molecules to adopt an antiperiplanar conformation around the C−X single bond (the C═O double bond is in mutual antiperiplanar orientation with respect to the X−C single bond forming the ring). The preferred conformation in noncyclic oxo- and thioesters is definitively synperiplanar.[27−29] Moreover, as a rule of thumb for cyclic compounds, the degree of strain energy parallels their reactivities.[30] This fact could be related to the changes observed in the product distribution when the size of the lactone rings varies. How these properties are related to and ultimately affect the stability of thiolactones have not been elucidated so far.

In the present work, the photochemical study of thietan-2-one (from now on, β-propiothiolactone) isolated in an argon matrix is reported. The matrixes were irradiated with broadband UV−visible radiation ($200 \leq \lambda \leq 800$ nm), and the photoproducts were identified on the basis of the IR spectra of the matrixes. In order to investigate the effect that structural and electronic properties exert on the photochemical behavior, the low-temperature X-ray diffraction pattern (measured using a laser-induced in situ crystallization method) and the gas-phase photoelectron spectra have been also obtained. The results were complemented by applying quantum chemical calculations at the B3LYP, MP2 and OVGF theories and employing 6-311++-G(d,p) and aug-cc-pVTZ basis sets. Finally, the strain energy was determined within the s-homodesmotic model including high-level MP2/6-311+G(2df,2pd) and the G2MP2 methods.

Experimental Section

Synthesis. β-Propiothiolactone was prepared by using benzyltriethylammonium tetrathiomolybdate as a sulfur-transfer reagent together with 3-bromopropionyl chloride, as was previously reported by Bhar et al.[31] In our case, the crude product was purified by repeated trap-to-trap condensation in vacuum. The final purity in both the vapor and liquid phase was carefully checked by reference to the IR, CG-MS, and ^{1}H and ^{13}C NMR spectra.[10]

Instrumentation. IR absorption spectra in the gaseous state were recorded with a resolution of 1 cm^{-1} in the range of 4000−400 cm^{-1} using a Bruker model EQUINOX 55 equipped with DLATGS detector (for the ranges 7500−370 cm^{-1}) with a KBr window.

A gas mixture of β-propiothiolactone with Ar was prepared in approximate compositions of X/matrix gas = 1:740 by standard manometric methods. The mixture was deposited on a CsI window cooled to ∼15 K by a Displex closed-cycle refrigerator (SHI-APD Cryogenics, model DE-202) using the pulsed deposition technique. The IR spectrum of the matrix sample was recorded at a resolution of 0.5 cm^{-1} and with 256 scans using a Nexus Nicolet instrument equipped with either an MCTB or a DTGS detector (for the ranges of 4000−400 cm^{-1} or 600−180 cm^{-1}, respectively). Following deposition and IR analysis of the resulting matrix, the sample was exposed to broadband UV−visible radiation ($200 \leq \lambda \leq 800$ nm) from a Spectral Energy Hg−Xe arc lamp operating at 800 W. The output from the lamp was limited by a water filter to absorb infrared radiation and therefore minimize any heating effects. The IR spectrum of the matrix was then recorded at different times of irradiation to analyze closely the decay and growth of the various absorptions.

The PE spectrum was recorded on a double-chamber UPS-II machine, which was designed specifically to detect transient species, as described elsewhere,[32,33] at a resolution of about 30 meV, indicated by the standard $Ar^+(^2P_{3/2})$ photoelectron band. Experimental vertical ionization energies were calibrated by simultaneous addition of a small amount of argon and methyl iodide to the sample.

An appropriate crystal of β-propiothiolactone of ∼0.3 mm diameter was obtained on the diffractometer at a temperature of 173(2) K with a miniature zone-melting procedure using focused infrared laser radiation.[34] The diffraction intensities were measured at low temperature on a Nicolet R3m/V four-circle diffractometer, intensities being collected with graphite-monochromatized Mo Kα radiation using the ω-scan technique. The structure was solved by Patterson syntheses and refined by full-matrix least-squares on F with the SHELXTL-Plus program.[35] Absorption correction details are given elsewhere. All atoms were assigned anisotropic thermal parameters. Atomic coordinates and equivalent isotropic displacement coefficients for heavy and hydrogen atoms are given in Tables S4 and S4 (Supporting Information), respectively, and anisotropic displacement parameters (Å$^2 \times 10^3$) for β-propiothiolactone are given in Table S4 (Supporting Information). X-ray crystallographic data in CIF format is given as Supporting Information. Crystal structure data have been deposited at the Cambridge Crystallographic Data Centre (CCDC). Enquiries for data can be directed to Cambridge Crystallographic Data Centre, 12 Union Road, Cambridge, U.K. CB2 1EZ, (e-mail) deposit@ccdc.cam.ac.uk, or (fax) +44 (0) 1223 336033. Any request to the CCDC for this material should quote the full literature citation and the reference number 719364.

Quantum Chemical Calculations. The calculations were performed using the GAUSSIAN 03[36] program package. Full geometry optimizations were done by applying ab initio (MP2) and DFT (B3LYP) methods using the 6-311++G(d,p) and aug-cc-pVTZ basis set. The calculated vibrational properties corresponded in all cases to potential energy minima for which no imaginary frequency was found. The vertical ionization energies (Ev) were calculated according to Cederbaum's outer valence Green's function (OVGF) method[37,38] with the 6-311++G(d,p) basis set, based on the B3LYP/6-311++G(d,p) optimized geometry. The Mülliken population analysis was applied to assign the atomic charges for both neutral and radical−cationic forms.

The strain energy of the title compound has been calculated by applying the s-homodesmotic approach introduced by Zhao and Gimarc.[39] To obtain the energies for all acyclic systems, optimum equilibrium geometries were computed for the singlet ground states of all pertinent molecular systems using B3LYP and MP2 methods with the 6-311++G(d,p) basis set. Several conformations were computed in order to ensure that the lowest-energy conformation was obtained for each molecular system. For each conformation, harmonic vibrational frequencies were also calculated at the same level of computation to ensure that

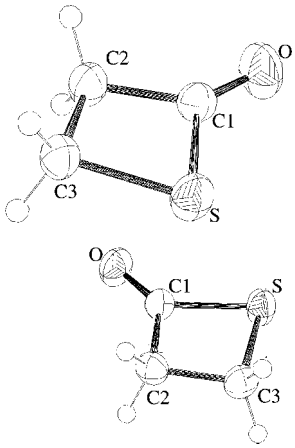

Figure 1. Molecular model with atom numbering for the single-crystal structure of β-propiothiolactone.

each optimized geometry corresponds to a true local minimum and to obtain the zero-point energy correction (ZPE). In all cases, electronic energies plus the zero-point energy were used to compute the strain energies. Additionally, electronic energies of the resulting minima were recalculated using single-point energy calculations of the MP2/6-311+G(2df,2pd) level. Finally, the strain energy was obtained with the high-level composite method G2MP2.[40,41]

Results

Crystal Structure. Because thiolactones of small ring size are liquids at ambient temperatures, the information about their structural characteristics is scarce. The development of special crystallization techniques has overcome this problem, making possible the extension of the studies to obtain solid-state information. By using the in situ laser-assisted crystallization technique developed in Essen,[34] an appropriate single crystal of β-propiothiolactone was grown at 178 K. The compound crystallizes in the monoclinic system, ($P2_1/c$ spatial group) with the following unit cell dimensions: a = 8.1062(1) Å, b = 10.3069(2) Å, c = 10.2734(1) Å, $\alpha = 90°$, $\beta = 107.628(1)°$, $\gamma = 90°$, and $Z = 8$ (for the full crystallographic data and treatment information, see Tables 1−4 in the Supporting Information). The structure of the molecule is shown in Figure 1, and Table 1 includes the main geometric parameters derived from the structure refinement, as well as those obtained from quantum chemical calculations. The overall crystal packing, as viewed along the *bc* plane, is shown in Figure 2.

There are two crystallographic nonequivalent molecules in the unit cell; consequently, each molecule crystallizes in a different packing environment. Geometrical parameters are almost the same, and both species have a planar structure with global molecular symmetry C_S. Molecules are arranged in layers separated from each other by 7.542 Å; the molecular planes form an angle of ∼30° with the crystallographic axis *c*. The contact distance between parallel layers is near 3.97 Å. The intermolecular interactions are dominated by O···H contacts, but also, there is evidence that short S···O=C and the C(3)···O=C contacts exist, whose distances are 3.279 and 3.120 Å, respectively (see Figure 1 for atom numbering).

In agreement with the experimentally determined structure, quantum chemical calculations predict a C_S molecular geometry, with a planar heavy atom skeleton for the title compound. For the oxygen analogues, gas electron diffraction[42,43] and microwave[43] investigations concluded that β-propiolactone has also a symmetry plane. In general, the results of the two methods that we have used to compute both bond lengths and bond angles compare well with the values obtained from the X-ray analysis. Both methods are less successful to reproduce the bond lengths around the sulfur atom. Thus, even with the large basis sets aug-cc-pVTZ, the B3LYP method overestimates the S−C bonds (by up to 0.02 Å for the S−C3 bond and 0.03 Å for the S−C1 bond). While these bonds are better described by the MP2 method with the modest 6-311++G(d,p) basis set, this method fails in reproduce the C=O double bond length and the ∠O=C−C bond angle parameters, which are calculated to be 0.02 Å longer and 1.1° smaller, respectively, than the experimentally determined values. Considering that the gas-phase structure can be approximated by the optimized molecular geometry (in a vacuum), relevant packing effects in solid β-propiothiolactone would seem to be absent.

Methyl thioacetate, $CH_3C(O)SCH_3$, is the direct acyclic thioester to be compared with β-propiothiolactone. The molecular structure of $CH_3C(O)SCH_3$ in the gas phase has been recently reported[44] and can offer a good frame of comparison between the molecular structure of cyclic and acyclic thioester compounds. Within this aim, geometrical parameters for the $CH_3C(O)SCH_3$ are also included in Table 1.

It should be noted first that GED for $CH_3C(O)SCH_3$ results in a structure with synperiplanar conformation (C=O double bond syn with respect to the S−C(H3) single bond),[44] a common feature observed for thioester species.[27−29,45,46] Due to steric reasons, short-chained cyclic thiolactones are forced to adopt an antiperiplanar conformation. Indeed, as is possible to compare in Table 1, remarkable differences between geometrical parameters of β-propiothiolactone and $CH_3C(O)SCH_3$[44] are observed. For example, the ∠C−S−C bond angle in β-propiothiolactone is 77.27(5)°, whereas in $CH_3C(O)SCH_3$, it is 99.2(9)°. On the other hand, the bond angles around the carbonyl group are higher in β-propiothiolactone; ∠O=C−S and ∠O=C−C amount to 131.25(9) and 134.20(11)°, respectively, whereas in $CH_3C(O)SCH_3$,[44] these values are 122.8(5) and 123.4(8)°, respectively. The associated endocyclic ∠C2−C1S bond angle is accordingly more acute in β-propiothiolactone [94.55(7)°], far apart from the ideal value of 120° for an sp^2-hybridized carbon atom. As expected, it becomes apparent that the ring strain has a major role in the structural properties of the title species.

Strain Energy. The trend in the molecular strain produced by decreasing the ring size in cyclic molecules is well-known.[47] The most important contributions to the ring strain are bond angle distortions (angular strain), bond stretching or compressions, repulsions between eclipsed hydrogen atoms (conformational strain), and torsions.[48] In particular, strain energies calculated for a series of four-membered species show that the angle distortion has an important effect on the stability of 1,2-cyclobutadiene and 1,2,3-cyclobutatriene.[49] The effect upon ring strain energy of the substitution of functional groups into small size rings has been discussed recently.[50] The influence on the strain energy of the formal introduction of an oxygen atom in the cycle or even a C=O group have been shown to be not relevant. However, an entirely different effect for second row elements has been reported. For instance, the substitution of a CH_2 group by a sulfur atom reduces the strain energy of cyclopropane by ∼8 kcal/mol.[50] In agreement with this trend, it was reported that the introduction of a C=O group into the three-membered ring hydrocarbon has little impact upon the strain energy, whereas the replacement of a methylene group by a sulfur atom reduces the strain energy.[50]

TABLE 1: Experimental and Calculated Geometric Parameters for the β-Propiothiolactone along with Experimentally Determined Gas-Phase Parameters for Methyl Thioacetate

		B3LYP			
parameter[a]	X-ray[b]	6-311++G(d,p)	aug-cc-pVTZ	MP2 6-311++G(d,p)	$CH_3C(O)SCH_3$[c]
r C1−C2	1.5163 (16)	1.5242	1.5213	1.5272	1.499(5)
r C2−C3	1.5340 (16)	1.5455	1.5425	1.5448	
r C3−S	1.8299 (12)	1.8558	1.8503	1.8356	1.805(6)
r C1−S	1.7913 (11)	1.8232	1.8189	1.8009	1.781(6)
r C=O	1.1813 (15)	1.1902	1.1892	1.1989	1.214(3)
∠C1SC3	77.27 (5)	76.43	76.64	76.63	99.2(9)
∠C1C2C3	95.68 (9)	95.71	95.91	94.43	
∠C2C3S	92.42 (7)	92.93	92.75	93.48	
∠C2−C1−S	94.55 (7)	94.93	94.70	95.47	113.8(9)
∠O=C−S	131.25 (9)	131.54	131.83	131.39	122.8(5)
∠O=C−C	134.20 (11)	133.53	133.47	133.15	123.4(8)

[a] See Figure 1 for atom numbering. [b] Uncertainties are σ values. [c] Gas-phase structure taken from ref 44.

Because the strain ring seems to affect significantly the molecular structure, the strain energy of β-propiothiolactone has been computed within the isodesmic, homodesmotic, and hyperhomodesmotic models, also called the s-homodesmotic approach.[39,51] The formal reactions needed for computation of the ring strain for β-propiothiolactone within this model are given in eqs 1−3.

Isodesmic Reaction:

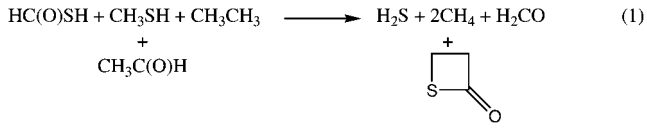

Homodesmotic Reaction:

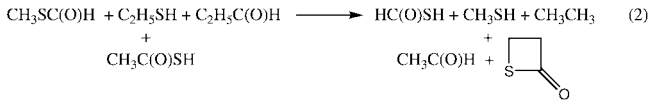

Hyperhomodesmotic Reaction:

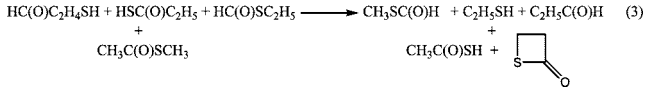

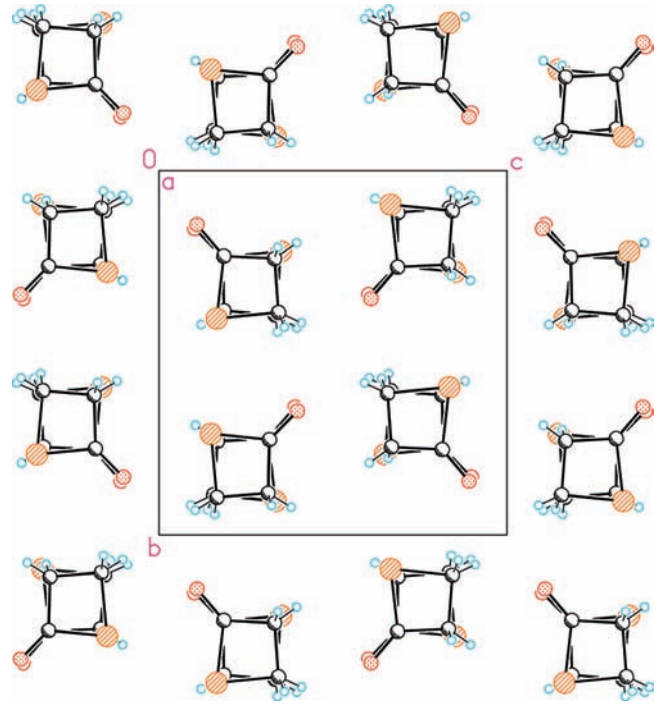

Figure 2. Stereoscopic illustration of the crystal packing of β-propiothiolactone at 178 K.

The conventional strain energies determined with the B3LYP and MP2 methods including zero-point corrections are listed in Table 2. Higher-order electronic correlation effects were found to be important in the computation of the strain energy of four-membered heterocyclic ring systems involving oxazirdine and its isomers.[52] Thus, in order to evaluate very accurate energies, the G2MP2 method was also employed to determine the strain energies.

As has been recently reported by Ringer and Magers[51] for cyclobutane, homodesmic and hyperhomodesmic models result in very similar strain energy values, whereas the isodesmic reaction scheme yields strain values which are definitively too low. These authors also pointed out that the B3LYP method underestimates the strain energy. All of these comments apply for our calculations on the strain energy of β-propiothiolactone. Moreover, by comparison of the MP2 results obtained with the 6-311++(d,p) and with the larger 6-311+G(2df,2pd) basis sets, a significant basis set effect is not noticed. The MP2 average values of 16.6 and 16.8 kcal/mol for the homodesmotic and hyperhomodesmotic methods, respectively, are in close agreement with the strain energies calculated at the G2MP2 level of approximation with values of 15.8 and 16.4 kcal/mol within the same reaction schemes, respectively.

Most studies of ring strain have centered on cyclobutane, which is the prototypical system for four-membered species.[50,51,53] The recommended experimental strain energy value for cyclobutane is 26.3 kcal/mol.[54] Similar values, 26.7 and 27.2 kcal/mol, were calculated by Bachrach using the group equivalent and hyperhomodesmotic approaches, respectively, at the CCSD(T)/6-311+G(2df,2pd) level.[53] The presence of a carbonyl group has little impact upon the strain energy of cyclobutanone, with calculated values of 28.7 kcal/mol. On the other hand, the replacement of a methylene group by a divalent sulfur atom reduces the strain of the ring, and thus, the thermochemically determined strain enthalpy of thietane is only 19.5 kcal/mol.[55,56] The calculated (CBS-Q) strain energy value determined for β-propiolactone is 22.7 kcal/mol.[50] The MP2/6-311+G(2df,2pd) calculated strain energy for β-propiothiolactone (16.64 kcal/mol) is lower than that calculated for cyclobutane (27.43 kcal/mol) at the same level of approximation and using the hyperhomodesmotic approach.[51] Thus, the observed tendency for the strain energy of the four-membered species here

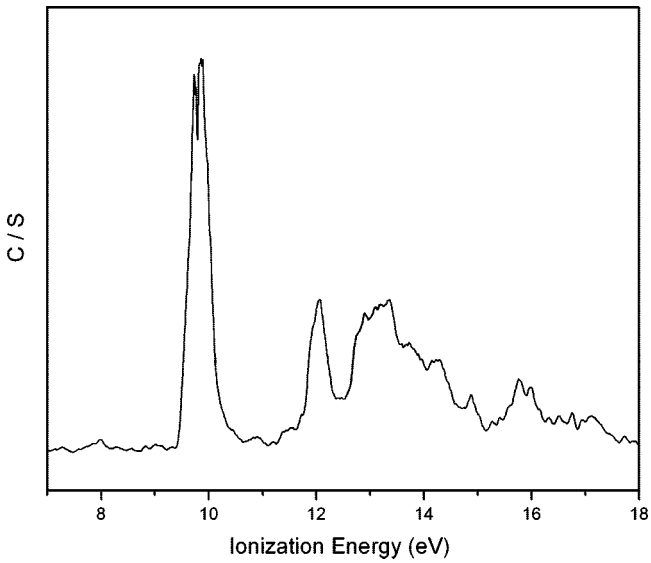

Figure 3. Photoeletron spectrum of β-propiothiolactone.

TABLE 2: Strain Energies (kcal/mol) for β-Propiothiolactone Determined within the Hyperhomodesmotic Model Using B3LYP, MP2, and G2MP2 Levels of Approximation

	B3LYP	MP2		
	6-311++G (d,p)	6-311++G (d,p)	6-311+G (2df,2pd)	G2MP2
isodesmic	5.75	3.19	2.56	3.94
homodesmotic	13.53	16.52	16.76	15.81
hyperhomodesmotic	12.11	17.12	16.64	16.43

considered is cyclobutanone ≅ cyclobutane > β-propiolactone > thietane > β-propiothiolactone.

He I Photoelectron Spectra. As was previously commented, the title compound belongs to the C_S symmetry point group. This fact allows us to classify the molecular orbitals as orbitals in plane with a′ symmetry and out of plane with a″ symmetry. This classification is extremely useful for the assignment of the bands observed in the PE spectra. The PE spectrum of β-propiothiolactone is presented in Figure 3. The experimentally observed ionization energies (IP in eV), calculated vertical ionization energies at OVGF/6-311++G(d,p) (Ev in eV), molecular orbitals, and molecular characters are summarized in Table 3.

Two bands appear overlapped at 9.73 and 9.87 eV; their narrow and sharp contours are characteristic of ionization from essentially nonbonding orbitals, which suggests these bands are associated primarily with the ionization of sulfur and oxygen lone-pair electrons (n_S, n_O) of the −SC(O)− group, with a″ and a″ symmetries, respectively. This fact is in agreement with the results of ab initio calculations, with respect to the ordering of the orbitals, as shown in Table 3, and also with the result obtained for the γ-butirothiolactone,[19] the five-membered ring analogue. For the first band (n''_S), the value observed for the vertical ionization (9.73 eV) is in good agreement with the theoretically predicted value of 9.44 eV [ROVGF/6-311++G(d,p)]. The adiabatic ionization energy derived from UB3LYP/6-311++G(d,p) is 9.32 eV.

There is a relatively large gap between the second and the third band, the latter having an IP of 12.06 eV. The calculations predict that this third band is associated with an ionization process from the π_{CO} orbital. After a second gap, a group of overlapping bands between 13 and 16 eV appears, which can be assigned to ionizations from the σ_{CH2} orbitals including the

TABLE 3: Experimental Vertical Ionization Energies (IP in eV), Computed Ionization Energies (Ev in eV) at the OVGF/6-311++G(d,p) Level of Approximation, and Molecular Orbital Characters for β-Propiothiolactone

IP (eV)	Ev (eV)[a]	MO	character
9.73	9.44	(23)	n''_S
9.87	9.89	(22)	n'_O
12.06	12.03	(21)	$\pi_{C=O}$
13.34	13.32	(20, 19)	$\sigma' + \sigma''_{C2-H's}$
13.74	13.63		
14.27	14.38	(18, 17)	$\sigma' + \sigma''_{C3-H's}$
	15.30		

[a] Molecular geometry calculated at the B3LYP/6-311++G(d,p) level.

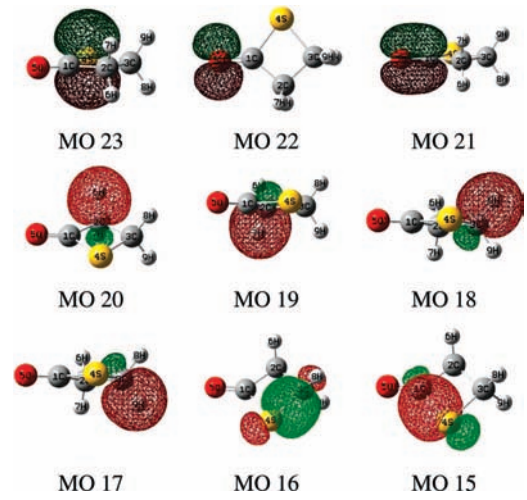

Figure 4. Drawings of nine HOMOs (highest occupied molecular orbitals) of β-propiothiolactone.

in-plane and out-of-plane types, as predicted by the calculations and depicted in Figure 4.

Further calculations (UB3LYP/6-311++G**) were performed in order to analyze the nature of the cation formed in the first ionization process. The results demonstrate that the atomic charges are mostly delocalized all over the molecule, with an appreciable fraction localized at the −C(O)S− group, as is listed in Table 4. The cyclic planar (C_S) molecular geometry is conserved after the ionization. The C1−S bond length is 0.46 Å longer, while the C=O double bond becomes 0.05 Å shorter in the cationic state. Vibrational calculations performed for the cationic form result in a large blue shift of 307 cm^{-1} for the $\nu_{C=O}$, while the ν_{C-S} exhibits a red shift of 32 cm^{-1} as compared with the neutral form.

Correlation Diagrams. Isaksson and Lijefors studied the photoelectron spectra of five-, six-, and seven-membered cyclic oxamides.[57] In these compounds, the oxamide unit is forced to adopt a different conformation than those preferred for equivalent unconstrained species. Thus, by comparing the ionization energies of cyclic and acyclic species, the influence on the electronic properties of the conformational change and strain energy can be inferred. Following this idea, the first three IPs of the β-propiothiolactone are correlated with the corresponding values determined for *S*-methyl thioacetate[58] and γ-butirothiolactone[19] in the diagram shown in Figure 5. The prominent features are the downward shifts in the n''_S and n'_O levels for β-propiothiolactone and the upward shifts in the $\pi_{C=O}$ levels in going from methyl thioacetate to γ-butirothiolactone. It was proposed that the interaction of the C=O group and the ring heteroatom in γ-butirothiolactone is primarily inductive in nature with negligible importance of electronic conjugation.[19] Resonance interactions in the −C(O)S− group are

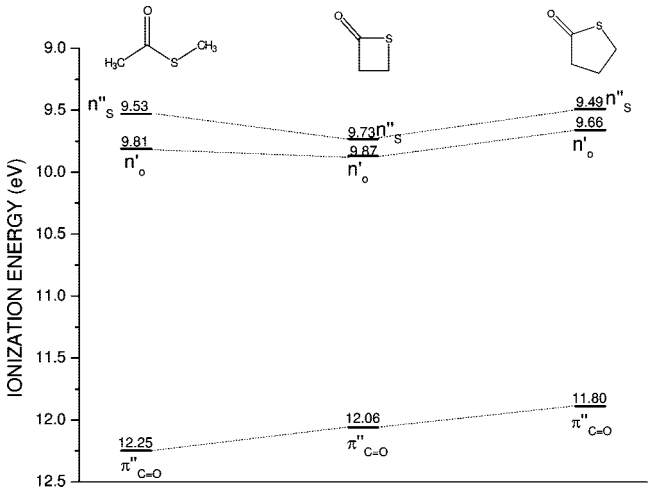

Figure 5. Correlation diagram of the ionization potentials of methyl thioacetate, β-propiothiolactone, and γ-butirothiolactone.

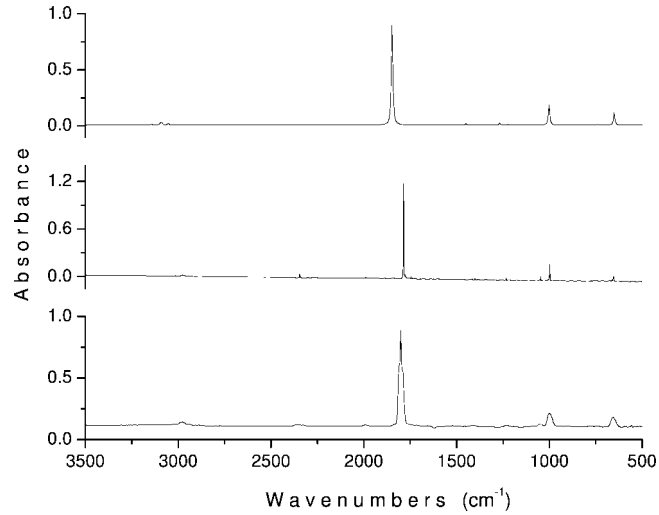

Figure 6. (Top) Calculated vibrational spectrum with B3LYP/aug-cc-pVTZ. (Middle) FTIR spectrum of an Ar matrix containing β-propiothiolactone following sample deposition. (Bottom) Gas IR spectrum at 2.0 mbar (glass cell, 100 mm optical path length, Si windows, 0.5 mm thick).

dominated by the out-of-plane (a″) $\pi^*_{C=O}$ and n''_S orbitals.[59] The nonplanarity of the five-membered thiolactone ring would prevent this interaction. The three outermost orbitals are less stabilized in the five-membered thiolactone as compared with the four-membered species. However, the trend observed in Figure 5 for $\pi_{C=O}$ is disrupted by comparing γ-butirothiolactone and β-propiothiolactone with the acyclic $CH_3C(O)SCH_3$ molecule. Thus, in order to consider the most important intramolecular interactions present in these species, the donor→ acceptor interaction energies for β-propio- and γ-butirothiolactones, and $CH_3C(O)SCH_3$ have been evaluated by using the NBO population analysis. Two energetically relevant interactions around the −SC(O)− group were specially analyzed,[59,60] (a) "mesomeric interaction" or the charge transfer from the lone-electron pair with π symmetry (n''_S) to the $\pi^*_{C=O}$ formally vacant orbital, which is a measure of the delocalization within the −SC(O)− fragment, and (b) "anomeric interaction" or the charge transfer from the in-plane p-type lone electron pair of the sulfur atom (n'_S) to the σ^*_{C-C} antibonding orbital. For *syn*-$CH_3C(O)SCH_3$, the corresponding acceptor is the $\sigma^*_{C=O}$ antibonding orbital.[59] At the B3LYP/6-311++G(d,p) level, these NBO interactions are nearly energetically equal in both the acyclic and cyclic studied compounds. For instances, the $n''_S \rightarrow \pi^*_{C=O}$ electronic interactions calculated for the syn and anti conformers of $CH_3C(O)SCH_3$ are 31.0 and 28.5 kcal/mol, respectively. Quite similar interaction energies were obtained for the thiolactone species, with values of 27.9 and 28.8 kcal/mol for β-propio and γ-butirothiolactone, respectively. These results clearly show that the resonance interaction is not affected by the nonplanarity of the thiolactone ring. The local planar symmetry around the carbonylic $C(sp^2)$ atom found in all of these compounds results in an efficient electronic conjugation.

Vibrational Analysis. Vibrational properties of β-propiothiolactone were investigated in detail by Kuz'yants,[10] who reported the Raman spectrum of the liquid and IR spectra of the gas, liquid, and crystals, together with an assignment of the fundamental vibrational modes. Since we are interested in the photochemical behavior of matrix-isolated β-propiothiolactone, an unambiguous interpretation of the matrix IR spectrum becomes interesting in the present study. The wavenumbers of the IR in the gaseous state, IR absorptions and intensity observed for a sample of the compound isolated in an Ar matrix at ∼15 K, and the theoretical vibrational wavenumbers calculated with the B3LYP/aug-cc-pVTZ method are presented as Supporting Information. A very good agreement between the experimental and theoretical spectra supports the full assignment of the observed bands. This agreement is demonstrated in Figure 6, where the gas-phase and argon matrix IR spectra are shown, together with the calculated IR spectrum at the B3LYP/aug-cc-pVTZ level. The new results are consistent with the earlier ones[10] and reveal significantly more details, giving confidence to the proposed band assignment.

UV−Visible Induced Photochemistry in Low-Temperature Inert Matrixes. After deposition, the Ar matrix was exposed to broadband UV−visible radiation ($200 \leq \lambda \leq 800$ nm) for different irradiation times ranging from 10 to 510 s, and the IR spectrum was measured at each stage. Table 5 lists the wavenumbers of all of the IR absorptions that develop upon photolysis. To distinguish the bands corresponding to the different species and to determine the sequence of the changes, the integrated intensities of the new bands have been plotted as a function of irradiation time, as depicted in Figure 7.

Most of the new bands exhibit the same pattern of growth. The most intense of these new bands occurs at 2136.3 cm^{-1} (see Figure 8a). At a first look, this observation might suggest the presence of a CO molecule[61] formed following a decarbonylation channel, in a comparable way as γ-butirothiolactone decomposes under thermal conditions[17,18] (Scheme 1). However, from previous results, it is well-known that ketenes also strongly absorb in this region.[62−64] In the present case, both ketene ($H_2C{=}C{=}O$) and methylketene ($CH_3CH{=}C{=}O$) could be formed in accordance with eqs 4 and 5.

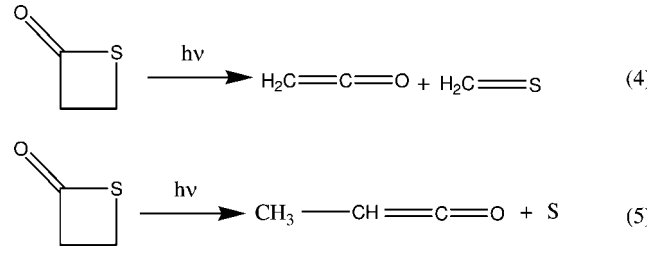

Indeed, the distinction between ketenes and CO by using infrared spectroscopy is a nontrivial problem because the $\nu(^{12}C{=}O)$ fundamental in both molecules could be coincident. To distinguish between them, the analysis of the satellite

TABLE 4: Mülliken Atomic Charges for the Molecular and Cation Radical Form of β-Propiothiolactone Calculated with the UB3LYP/6-311++G(d,p) Approximation

	atoms[a]						
	C1	C2	C3	S	O	H (av)	TAC[b]
$C_2H_4C(O)S$	0.191	−0.550	−0.172	0.062	−0.235	0.176	0
$C_2H_4C(O)S^+$	0.528	−0.691	−0.201	0.329	−0.026	0.265	+1
Δq[c]	0.337	−0.141	−0.029	0.267	0.209	0.089	+1

[a] See Figure 1 for atom numbering. [b] Total atomic charge, [c] $\Delta q = q(C_2H_4C(O)S^{\bullet+}) - q(C_2H_4C(O)S)$.

TABLE 5: Wavenumbers, Intensities, and Assignments of the IR Absorptions Appearing after 510 sec of Broadband Photolysis of β-Propiothiolactone in an Ar Matrix

IR		assignment		
ν [cm^{-1}]	I	molecule	vibrational mode	wavenumber reported previously
3549.6	0.056	$CH_3CH{=}C{=}O$[67]	$\nu(C{=}O) + \rho(CH_3)$	
3503.8	0.003	$CH_3CH{=}C{=}O$[67]	$\nu(C{=}O) + \delta(CH_3)$	
3161.8	0.011	$CH_3CH{=}C{=}O$[67]	$\nu(C{=}O) + CH_3$ wag	
3071.3	0.018	$CH_2{=}CH_2$[72−74]	$\nu(CH_2)(B_{1g})$	3081
3065.8	0.017	$CH_3CH{=}C{=}O$[67]	$\nu_s(CH_2)$	3069
3006.2	0.003	C_2H_4S[70]	$\nu(CH_2)(A_1) + \nu(CH_2)(B_2)$	3013.5
2994.1	0.001	$CH_2{=}CH_2$[72−74]	$\nu(CH_2)(B_{3u})$	2995
2974.1	0.006	$CH_3CH{=}C{=}O$[67]	$\nu_{as}(CH_3)(a'')$	2966
2906.1	0.008	$CH_3CH{=}C{=}O$[67]	$\nu(CH_2)(a')$	2912.1
2874.7	0.002	$CH_3CH{=}C{=}O$[67]	$\nu(CH_2)(a')$	2874
2140.6	0.274	CO[61]	$\nu(C{=}O)$	2137.9
2138.5	0.207	$CH_3CH{=}C{=}O$[67]		2138.0
2136.3	0.756			
2127.0	0.025		$\nu_{as}(C{=}C{=}O)$	2129.1
2121.7	0.010			2125.2
2089.7	0.002	CO[62]	$\nu(^{13}C{=}O)$	2090.0
2079.9	0.007	$CH_3CH{=}C{=}O$[67]	$\nu(^{13}C{=}O)$	2075.3
2051.8 sh		OCS[62,71]		
2050.6	0.416			
2048.9 sh			$\nu(C{=}O)$	2049.6
2046.5	0.093			
1597.6	0.036	$CH_2{=}CH_2$?		
1441.9	0.002	$CH_3CH{=}C{=}O$[67]	$\delta(CH_3)(a')$	1470.7 1447.3
1439.6	0.005	$CH_3CH{=}C{=}O$[67]	$\rho(CH_3)$	1447
1433.9	0.013	$CH_2{=}CH_2$[72−74]	CH_2 sciss (B_{3u})	1440 1438
1428.1	vw			
1374.5	0.029	$CH_3CH{=}C{=}O$[67]	$\delta(CH_3)$	1388.3 1382.9 1377.1
1357.3	0.056			
1355.4	0.029			
1349.8	0.027	$CH_2{=}CH_2$[72−74]	CH_2 sciss (A_g)	1343
1346.1	0.009			
1344.8	0.053			
1343.1	0.006			
1146.2	0.015	$CH_3CH{=}C{=}O$[67]	δ (CCH)	1155
1066.4	0.008	$CH_3CH{=}C{=}O$[67]	$\nu_s(C{=}C{=}O)$	1063
1064.2	0.011			
1049.0	0.002	$CH_3CH{=}C{=}O$[67]	$\rho(CH_3)$	1043
1047.1	0.003			
972.6	0.010			
949.1	0.027	$CH_2{=}CH_2$[74]	$(CH_2)(B_{1u})$ wag	946
869.5	0.009	$CH_3CH{=}C{=}O$[67]	CH_3 wag	886
858.0	0.001	OCS		
624.5	0.031	C_2H_4S[70]	$\nu(C{-}S)(B_2)$	627.3
519.3	0.045	$CH_3CH{=}C{=}O$[67]	γ (CO) oop	521.0

absorptions corresponding to $\nu(^{13}C{=}O)$ has been proposed.[62] The very strong absorption at 2136.3 cm^{-1} is accompanied by a satellite at 2079.9 cm^{-1} with an intensity reflecting the natural abundances of ^{12}C and ^{13}C (∼100:1). Such a low wavenumber value for the $\nu(^{13}C{=}O)$ fundamental suggests that a ketene species is formed predominantly.[65] To distinguish between the formation of ketene and/or methylketene, a detailed comparison between the argon matrix spectra reported for pure samples of $H_2C{=}C{=}O$[66] and $CH_3CH{=}C{=}O$[67] was performed. Several features that might be assigned to these species become apparent in the product spectra. A clear distinction between ketene and methylketene, however, is rather difficult in the present case due the fact that the spectrum of the photolytically generated species is perturbed by the presence of a second photoproduct in the same matrix cage. Thus, since the production of ketene implies the concomitant formation of $H_2C{=}S$, absorptions expected for this molecule were analyzed according to previous references.[68,69] In particular, its $\nu(C{=}S)$ stretching mode, at ∼1200 cm^{-1}, should be unambiguously characterized. On this basis, the absence of the C=S stretching vibration of $H_2C{=}S$ reveals that $H_2C{=}C{=}O$ is also not a

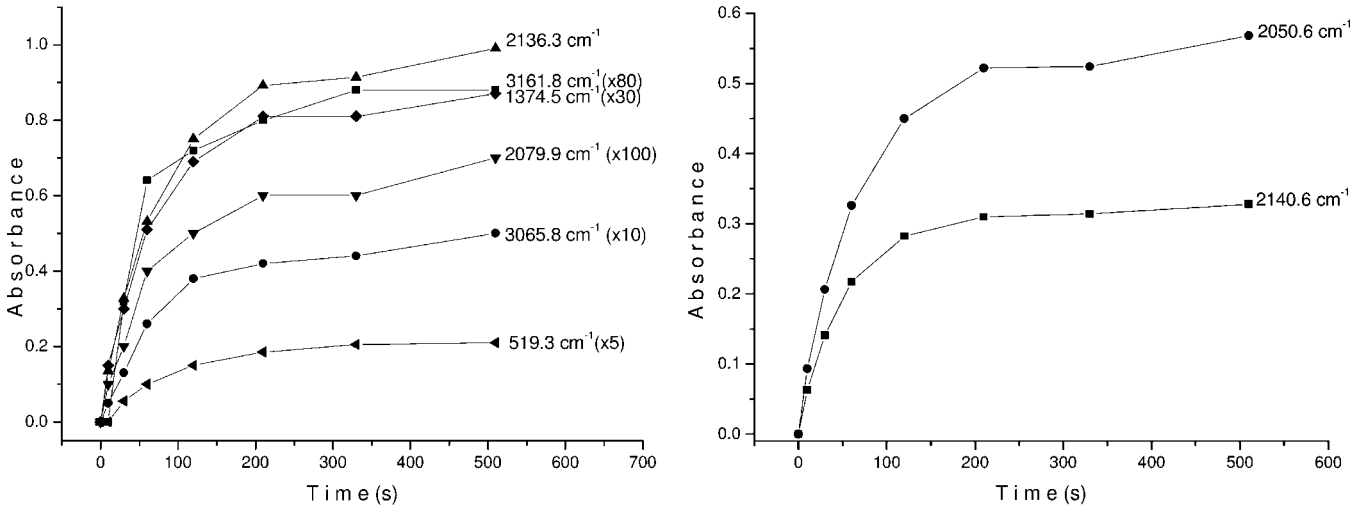

Figure 7. Plots as a function of irradiation time of the intensities of the bands assigned to $CH_3CH{=}C{=}O$ (left) CO and OCS (right) in the IR spectrum of an Ar matrix.

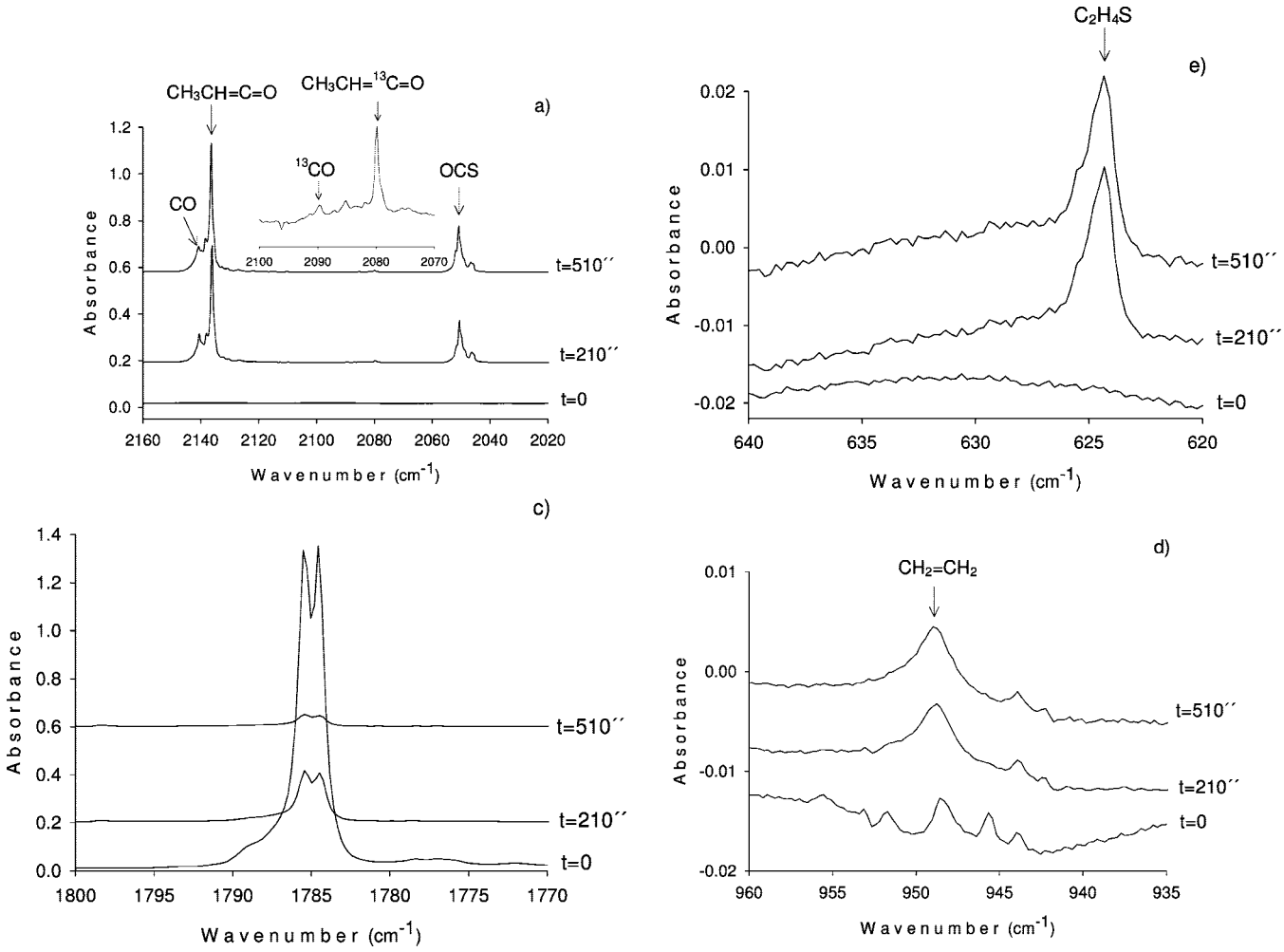

Figure 8. FTIR spectrum for an Ar matrix initially containing β-propiothiolactone at different irradiation times in the regions of (a) 2160−2020, (b) 640−620, (c) 1800−1770, and (d) 960−935 cm^{-1}.

photoproduct of matrix-isolated β-propiothiolactone upon broadband UV−vis irradiation.

Figure 8a shows that together with the strong absorption at 2136.3 cm^{-1}, other features with lower intensity grow at 2140.6, 2138.5, 2127.0, and 2121.7 cm^{-1} after photolysis. The most likely explanation of the new bands is that they arise from the $\nu(^{12}C{=}O)$ fundamental of methylketene molecules trapped in different sites in the rigid matrix cages.[67] Nevertheless, the presence of minor quantities of carbon monoxide cannot be ruled out. In effect, the very low intensity band at 2089.7 cm^{-1} (see inset of Figure 8a) can be associated with the corresponding ^{13}C satellite for the $\nu(C{=}O)$ mode of free CO. The main $\nu(^{12}CO)$ fundamental for CO could be either overlapped by that of the ketene or be tentatively assigned to the absorption observed at

2140.6 cm^{-1}. The later hypothesis is supported by the fact that the intensity of the band at 2089.7 cm^{-1} is roughly 1% of that at 2140.6 cm^{-1}. The formation of CO suggests that thiirane (C_2H_4S) is also formed following eq 6

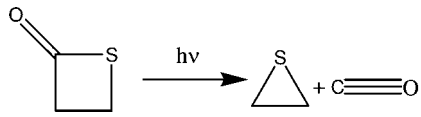

(6)

The identity of the thiirane product is confirmed by comparison with the gas-phase IR spectrum reported by Allen et al.[70] The most distinctive feature in the vibrational spectra of thiirane is the presence of a sharp band at 624 cm^{-1}, assigned to the ν_{as}(C−S) fundamental mode (see Figure 8b).

Another intense band is observed at 2050.6 cm^{-1}, which was assigned with confidence to the stretching (C═O) for the molecule of OCS (see Figure 7 right).[71] The formation of OCS suggests that ethene is also formed from β-propiothiolactone under the action of broadband UV−visible light in accordance with eq 7. Ethene was mainly identified by the evolution with the irradiation time of absorptions at 949.1 and 1441.9 cm^{-1}, assigned to the CH_2 wagging and scissor normal modes, respectively,[72−74] shown in Figure 8d. These correspond to the most intense absorptions in the CH_2═CH_2 matrix spectra.[72−74] Another very weak bands at 3071.3 and 2994.1 cm^{-1} could also correspond to the formation of CH_2═CH_2; however, because of band overlapping, a definitive assignment of these bands is not possible at this point.

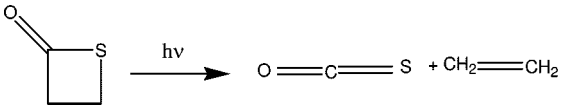

(7)

The formation of trace quantities of carbonylic compounds cannot be ruled out since very very low intensity features were observed in the carbonyl stretching region after irradiation. Figure 8c shows the 1800−1770 cm^{-1} carbonylic region, illustrating also that after 510 s of broadband UV−visible irradiation, almost all initial β-propiothiolactone was consumed.

Discussion

It is well-known that the gas-phase thermal decomposition of β-propiolactone yields ethylene and carbon dioxide in equal amounts as the only products.[21−24] The reaction is homogeneous, obeys a first-order kinetics, and occurs in a concerted fashion, via an activated complex with zwitterionic character.[26] The products are those expected on the thermochemical basis. Thus, the lower-energy process takes place exclusively. No traces of ketene, acetaldehyde, or carbon monoxide have been identified,[21−24] and only a minor heterogeneous isomerization to acylic acid [CH_2═CHC(O)OH] has been reported.[26] Moreover, the result obtained in the study of IR multiple photon decomposition of β-propiolactone in the gas phase suggests that the same decomposition channel occurs for the compound at highly excited vibrational states.[75,76]

On the other hand, the photoinduced decompositions of lactones are very complex processes. For instance, the photodecomposition of γ-butyrolactone has been studied in the vapor phase at 125 °C with 210−260 nm radiation. The reported photoproducts are C_2H_4, CO, H_2C═O, the isomeric species succinaldehyde, cyclopropane (c-C_3H_6), propylene (C_3H_6), and CO_2.[77] The product distribution changes with the energy of the incident radiation; at longer wavelengths, the formation of c-C_3H_6 and C_3H_6 is favored. On the other hand, thermal decomposition experiments showed that C_2H_4 is the major photoproduct. C_3H_6, c-C_3H_6, and succinaldehyde have been not detected.[78]

To the best of our knowledge, neither thermal- nor photoinduced studies on the four-membered sulfur analogues have been reported so far. However, the UV-induced photochemistry of five-membered species 2(*5H*)-furanone and 2(*5H*)-thiophenone isolated in low-temperature inert matrixes has been very recently reported by Breda et al.[16] Both compounds can be found to undergo α-cleavage upon low-energy UV irradiation but at different excitation wavelengths. The open ring aldehyde−ketene molecule can be generated at higher energies than the sulfur analogues (thioaldehyde−ketene). At higher excitation energies (λ > 235 nm), the latter species can be further transformed into the closed-ring Dewar isomer, whereas the aldehyde−ketene is photostable under these conditions. Their different photochemical reactivity could be attributed to a considerable reduction of the HOMO−LUMO ($n''_S-\pi^*_{C=O}$) gap in the sulfur-containing species, as deduced from a natural bond orbital analysis. The photoelectron spectra of 2(*5H*)-thiophenone was reported by Chin et al.[79] While the frontier orbitals correspond to the n''_S (9.63 eV) and n'_O (9.75 eV) lone-electron pairs, a singular stabilization of the $\pi_{C=O}$ was found, with ionization potential value of 14.10 eV, explained in terms of a strong resonant interaction between the C═O and C═C groups. These studies could serve as a starting point to compare the photochemical evolution of carbonyl heterocyclic compounds containing either oxygen or sulfur atoms in the ring. The similarity between the techniques used (matrix photochemistry and photoelectron spectroscopy) is another noticeable advantage.

According to the results obtained in the study of the photoelectron spectra, the outermost orbitals of β-propiothiolactone are formally located at the −SC(O)− group, n''_S, n'_O, and $\pi_{C=O}$, with ionization energies of 9.73, 9.87, and 12.06 eV, respectively. Moreover, it is well-known that the LUMO in the thioester moiety corresponds to the $\pi^*_{C=O}$ antibonding orbital. The UV−visible spectra of unsubstituted thiolactones and thioesters are dominated by strong $\pi \rightarrow \pi^*$ transitions, while the $n \rightarrow \pi^*$ transition occurs as a low-intensity band, overlapped with the former. The lower levels of virtual orbitals, such as σ^*_{C-S} for bivalent sulfur atoms, have been also emphasized.[80] The calculated LUMO for the title compound corresponds, as expected, to the $\pi^*_{C=O}$ antibonding orbital. Thus, it is apparent that the −SC(O)− moiety acts as a chromophore in thiolactones, and the UV−visible exited electronic states should be associated with excitations from the n''_S, n'_O, and $\pi_{C=O}$ to vacant molecular orbitals with strong antibonding characters on this set.

The matrix photochemistry of β-propiothiolactone is characterized by the formation of methylketene together with the extraction of a sulfur atom as the major decomposition channel, where the rupture of the carbon−sulfur bonds (C1−S and C3−S) is involved. Following in importance, another photoevolution process involving the formation of OCS and ethene proceeds simultaneously. Thus, the reaction mechanisms seem to imply a ring-opening reaction, and the rupture of a second bond remains as the open question about the concerted or consecutive nature of this pathway.

Conclusion

The matrix photochemistry of β-propiothiolactone is characterized by the formation of methylketene as the major

decomposition channel. To the best of our knowledge, such a dissociation process (thermally or photochemically induced) leading to a ketene derivative has not been previously reported for thiolactones. These results contrast with those reported for the gas-phase pyrolysis of the five-membered analogue species, γ-butyrothiolactone, where decarbonylation is the main reaction channel. Thus, it is expected that important differences exist between the photochemical and thermal decomposition behavior of the title compound.

In addition to the identification of various decay products and the different decomposition pathways leading to them, the present study has also been concerned with the electronic and molecular structure of β-propiothiolactone. These results corroborate that the ring strain affects both structural and valence electronic properties of the title compound. These facts invite one to perform further investigations on higher-membered thiolactone analogues in order to compare the influence of the ring size and its associated ring strain energy on both thermal and photochemical behavior.

Acknowledgment. The authors are indebted to the Agencia Nacional de Promoción Científica y Tecnológica (ANPCyT), Consejo Nacional de Investigaciones Científicas y Técnicas (CONICET), and the Comisión de Investigaciones Científicas de la Provincia de Buenos Aires (CIC), República Argentina, for financial support. They also thank the Facultad de Ciencias Exactas, Universidad Nacional de La Plata, República Argentina for financial support. N.Y.D. and C.O.D.V. especially acknowledge the DAAD, which generously sponsors the DAAD Regional Program of Chemistry for the República Argentina supporting Latin−American students to make their Ph.D. in La Plata.

Supporting Information Available: Crystallographic details and listings of atomic coordinates and equivalent isotropic displacement coefficients and anisotropic displacement parameters for β-propiothiolactone are given in Tables S1−4; X-ray crystallographic data is also given. Table S5 lists the vibrational data of β-propiothiolactone including computed (B3LYP/aug-cc-pVTZ) and Ar matrix infrared data with a tentative band assignment. This material is available free of charge via the Internet at http://pubs.acs.org.

References and Notes

(1) Jakubowski, H. *FASEB J.* **1999**, *13*, 2277.
(2) Jakubowski, H. *J. Nutr.* **2000**, *130*, 377.
(3) Jakubowski, H. *J. Biol. Chem.* **1997**, *272*, 1935.
(4) Rowe, D. J. *Perfum. Flavor.* **1998**, *23*, 9.
(5) Roling, I.; Schmarr, H.-G.; Eisenreich, W.; Engel, K.-H. *J. Agric. Food Chem.* **1998**, *46*, 668.
(6) Alonso, J.; Lopez, J. *Z. Naturforsch.* **1982**, *37A*, 129.
(7) Alonso, J. L. *J. Chem. Soc., Chem. Commun.* **1981**, *12*, 577.
(8) Alonso, J. L.; Lopez, J. C.; Mata, F. *Z. Naturforsch.* **1981**, *37A*, 129.
(9) Deerfield, D. W., II.; Pedersen, L. G. *J. Mol. Struct.: THEOCHEM* **1995**, *358*, 99.
(10) Kuz'yants, G. M. *J. Struct. Chem.* **1975**, 696.
(11) Huang, H. H.; Fan, K. N.; Huang, W.; Li, Z. H.; Mok, C. Y.; Wang, W. N.; Chin, W. S. *Chem. Phys. Lett.* **1997**, *265*, 508.
(12) Lee, H. B.; Park, H.-Y.; Lee, B.-S.; Kim, Y. G. *Magn. Reson. Chem.* **2000**, *38*, 468.
(13) Padwa, A.; Dehm, D.; Oine, T.; Lee, G. A. *J. Am. Chem. Soc.* **1975**, *97*, 1837.
(14) Elke Anklam, P. M. *Angew. Chem., Int. Ed.* **1984**, *23*, 364.
(15) Breda, S.; Reva, I.; Fausto, R. *J. Mol. Struct.* **2008**, *887*, 75.
(16) Breda, S.; Reva, I.; Fausto, R. *Vib. Spectrosc.* In press.
(17) Rai-Chaudhuri, A.; Chin, W. S.; Mok, C. Y.; Huang, H.-H. *J. Chem. Res.* **1994**, 378.
(18) Rai-Chaudhuri, A.; Chin, W. S.; Kaur, D.; Mok, C. V.; Huang, H. H. *J. Chem. Soc., Perkin Trans. 2* **1993**, 1249.
(19) Chin, W. S.; Xu, Z. P.; Mok, C. Y.; Huang, H. H.; Mutoh, H.; Masuda, S. *J. Electron Spectrosc. Relat. Phenom.* **1998**, *88*−*91*, 97.
(20) Bailey, W. J.; Bird, C. N. *J. Org. Chem.* **1977**, *42*, 3895.
(21) Noyce, D. S.; Banitt, E. H. *J. Org. Chem.* **1966**, *31*, 4043.
(22) Adam, W.; Baeza, J.; Liu, J.-C. *J. Am. Chem. Soc.* **1972**, *94*, 2000.
(23) Holbrook, K. A.; Scott, R. A. *J. Chem. Soc., Faraday Trans. 1* **1975**, *71*, 1849.
(24) James, T. L.; Wellington, C. A. *J. Am. Chem. Soc.* **1969**, *91*, 7743.
(25) Safont, V. S.; Andrés, J.; Domingo, L. R. *Chem. Phys. Lett.* **1998**, *288*, 261.
(26) Frey, H. M.; Pidgeon, I. M. *J. Chem. Soc., Faraday Trans. 1* **1985**, *81*, 1087.
(27) Ulic, S. E.; Della Védova, C. O.; Hermann, A.; Mack, H.-G.; Oberhammer, H. *J. Phys. Chem. A* **2008**, *112*, 6211.
(28) Gobbato, K. I.; Della Védova, C. O.; Mack, H. G.; Oberhammer, H. *Inorg. Chem.* **1996**, *35*, 6152.
(29) Erben, M. F.; Boese, R.; Della Védova, C. O.; Oberhammer, H.; Willner, H. *J. Org. Chem.* **2006**, *71*, 616.
(30) Huisgen, R. *Angew. Chem., Int. Ed.* **1986**, *25*, 297.
(31) Bhar, D.; Chandrasekaran, S. *Tetrahedron* **1997**, *53*, 11835.
(32) Geronés, M.; Erben, M. F.; Romano, R. M.; Della Védova, C. O.; Yao, L.; Ge, M. *J. Phys. Chem. A* **2008**, *112*, 2228.
(33) Zeng, X. Q.; Liu, F. Y.; Sun, Q.; Ge, M. F.; Zhang, J. P.; Ai, X. C.; Meng, L. P.; Zheng, S. J.; Wang, D. X. *Inorg. Chem.* **2004**, *43*, 4799.
(34) Boese, R.; Nussbaumer, M. In situ Crystallization Techniques. In *Organic Crystal Chemistry*; Jones, D. W., Ed.; Oxford University Press: Chichester, U.K., 1994; Vol. 7; p 20.
(35) *SHELTX-Plus*, Version SGI IRIS Indigo, a Complex Software Package for Solving, Refining and Displaying Crystal Structures, Siemens: Germany; 1991.
(36) Frisch, M. J.; Trucks, G. W.; Schlegel, H. B.; Scuseria, G. E.; Robb, M. A.; Cheeseman, J. R.; Montgomery, J. A., Jr.; Vreven, T.; Kudin, K. N.; Burant, J. C.; Millam, J. M.; Iyengar, S. S.; Tomasi, J.; Barone, V.; Mennucci, B.; Cossi, M.; Scalmani, G.; Rega, N.; Petersson, G. A.; Nakatsuji, H.; Hada, M.; Ehara, M.; Toyota, K.; Fukuda, R.; Hasegawa, J.; Ishida, M.; Nakajima, T.; Honda, Y.; Kitao, O.; Nakai, H.; Klene, M.; Li, X.; Knox, J. E.; Hratchian, H. P.; Cross, J. B.; Bakken, V.; Adamo, C.; Jaramillo, J.; Gomperts, R.; Stratmann, R. E.; Yazyev, O.; Austin, A. J.; Cammi, R.; Pomelli, C.; Ochterski, J. W.; Ayala, P. Y.; Morokuma, K.; Voth, G. A.; Salvador, P.; Dannenberg, J. J.; Zakrzewski, V. G.; Dapprich, S.; Daniels, A. D.; Strain, M. C.; Farkas, O.; Malick, D. K.; Rabuck, A. D.; Raghavachari, K.; Foresman, J. B.; Ortiz, J. V.; Cui, Q.; Baboul, A. G.; Clifford, S.; Cioslowski, J.; Stefanov, B. B.; Liu, G.; Liashenko, A.; Piskorz, P.; Komaromi, I.; Martin, R. L.; Fox, D. J.; Keith, T.; Al-Laham, M. A.; Peng, C. Y.; Nanayakkara, A.; Challacombe, M.; Gill, P. M. W.; Johnson, B.; Chen, W.; Wong, M. W.; Gonzalez, C.; Pople, J. A. *Gaussian 03*, revision B.04; Gaussian, Inc.: Pittsburgh, PA, 2004.
(37) Cederbaum, L. S.; Schirmer, J.; Domcke, W.; von Niessen, W. *J. Phys. B* **1977**, *10*, L549.
(38) Cederbaum, L. S.; Domcke, W. *Adv. Chem. Phys.* **1977**, *36*, 205.
(39) Zhao, M.; Gimarc, B. M. *J. Phys. Chem.* **1993**, *97*, 4023.
(40) Curtiss, L. A.; Raghavachari, K.; Redfern, P. C.; Stefanov, B. B. *J. Chem. Phys.* **1998**, *108*, 692.
(41) Curtiss, L. A.; Raghavachari, K.; Pople, J. A. *J. Chem. Phys.* **1993**, *98*, 1293.
(42) Bregman, J.; Bauer, S. H. *J. Am. Chem. Soc.* **1955**, *77*, 1955.
(43) David, W. B.; Chester, O. B.; James, E. B. *J. Chem. Phys.* **1965**, *43*, 1190.
(44) Della Védova, C. O.; Romano, R. M.; Oberhammer, H. *J. Org. Chem.* **2004**, *69*, 5395.
(45) Erben, M. F.; Della Védova, C. O.; Willner, H.; Boese, R. *Eur. J. Inorg. Chem.* **2006**, *21*, 4418.
(46) Erben, M. F.; Della Védova, C. O.; Willner, H.; Trautner, F.; Oberhammer, H.; Boese, R. *Inorg. Chem.* **2005**, *44*, 7070.
(47) Kenneth, B. W. *Angew. Chem., Int. Ed.* **1986**, *25*, 312.
(48) Saiyasombat, W.; Molloy, R.; Nicholson, T. M.; Johnson, A. F.; Ward, I. M.; Poshyachinda, S. *Polymer* **1998**, *39*, 5581.
(49) Daoust, K. J.; Hernandez, S. M.; Konrad, K. M.; Mackie, I. D.; Winstanley, J.; Johnson, R. P. *J. Org. Chem.* **2006**, *71*, 5708.
(50) Bach, R. D.; Dmitrenko, O. *J. Am. Chem. Soc.* **2006**, *128*, 4598.
(51) Ringer, A. L.; Magers, D. H. *J. Org. Chem.* **2007**, *72*, 2533.
(52) Lewis, L. L.; Turner, L. L.; Salter, E. A.; Magers, D. H. *J. Mol. Struct.: THEOCHEM* **2002**, *592*, 161.
(53) Bachrach, S. M. *J. Org. Chem.* **2008**, *73*, 2466.
(54) Eliel, E. L.; Wilen, S. H. *Stereochemistry of Organic Chemistry*; John Wiley & Son: New York, 1994.
(55) Eicher, T.; Hauptmann, S.; Speicher, A. Four-Membered Heterocycles. In *The Chemistry of Heterocycles*, 2nd ed.; Wiley-VCH Verlag GmbH & Co.: New York, 2004; p 38.
(56) Stirling, C. J. M. *Tetrahedron* **1985**, *41*, 1613.
(57) Isaksson, R.; Liljefors, T. *J. Chem. Soc., Perkin Trans. 2* **1980**, 1815.

(58) Geronés, M.; Downs, A. J.; Erben, M. F.; Ge, M.; Romano, R. M.; Yao, L.; Della Védova, C. O. *J. Phys. Chem. A* **2008**, *112*, 5947.
(59) Erben, M. F.; Della Védova, C. O.; Romano, R. M.; Boese, R.; Oberhammer, H.; Willner, H.; Sala, O. *Inorg. Chem.* **2002**, *41*, 1064.
(60) Fausto, R. *J. Mol. Struct.: THEOCHEM* **1994**, *315*, 123.
(61) Romano, R. M.; Della Védova, C. O.; Downs, A. J. *J. Phys. Chem. A* **2004**, *108*, 7179.
(62) Romano, R. M.; Della Védova, C. O.; Downs, A. J. *J. Phys. Chem. A* **2002**, *106*, 7235.
(63) Johnston, D. E.; Sodeau, J. R. *J. Chem. Soc., Faraday Trans.* **1992**, *88*, 409.
(64) Winter, P. R.; Rowland, B.; Hess, W. P.; Radziszewski, J. G.; Nimlos, M. R.; Ellison, G. B. *J. Phys. Chem. A* **1998**, *102*, 3238.
(65) Bandow, H.; Akimoto, H. *J. Phys. Chem.* **1985**, *89*, 845.
(66) Moore, C. B.; George, C. P. *J. Chem. Phys.* **1963**, *38*, 2816.
(67) Harrison, J. A.; Frei, H. *J. Phys. Chem.* **1994**, *98*, 12142.
(68) Romano, R. M.; Della Védova, C. O.; Downs, A. J. *Chem.—Eur. J.* **2007**, *13*, 8185.
(69) Clouthier, D. J.; Ramsay, D. A. *Annu. Rev. Phys. Chem.* **1983**, *34*, 31.
(70) Allen, W. D.; Bertie, J. E.; Falk, M. V.; Hess, B. A. J.; Mast, G. B.; Othen, D. A.; Schaad, L. J.; Schaefer, H. F., III. *J. Chem. Phys.* **1986**, *84*, 4211.
(71) Hawkins, M.; Almond, M. J.; Downs, A. J. *J. Phys. Chem.* **1985**, *89*, 3326.
(72) Cowieson, D. R.; Barnes, A. J.; Orville-Thomas, W. J. *J. Raman Spectrosc.* **1981**, *10*, 224.
(73) Rytter, E.; Gruen, D. M. *Spectrochim. Acta, PartA* **1979**, *35*, 199.
(74) Barnes, A. J.; Howells, J. D. R. *J. Chem. Soc' Faraday Trans. 2* **1973**, *69*, 532.
(75) Yamamoto, S.; Ishikawa, Y.; Arai, S. *Bull. Chem. Soc. Jpn.* **1986**, *59*, 2241.
(76) Sugita, K.; Miyamoto, Y.; Arai, S.; Kuribayashi, S.; Majima, T.; Yamamoto, S. *J. Phys. Chem. A* **2000**, *104*, 2587.
(77) Simonaitis, R.; Pitts, J. N. *J. Phys. Chem.* **1971**, *75*, 2733.
(78) Braslavsky, S.; Heicklen, J. *Chem. Rev.* **1977**, *77*, 473.
(79) Chin, W. S.; Xu, Z. P.; Mok, C. Y.; Huang, H. H.; Mutoh, H.; Masuda, S. *J. Electron Spectrosc. Relat. Phenom.* **1998**, *88−91*, 97.
(80) Nagata, S.; Yamabe, T.; Fukui, K. *J. Phys. Chem.* **1975**, *79*, 2335.

JP811480V